

# Breakdown of broken-symmetry approach to exchange interaction

Naoya Iwahara,<sup>1,2, a)</sup> Zhishuo Huang,<sup>2,3</sup> Akseli Mansikkamäki,<sup>4</sup> and Liviu F. Chibotaru<sup>2, b)</sup>

<sup>1)</sup> Graduate School of Engineering, Chiba University, 1-33 Yayoi-cho, Inage-ku, Chiba-shi, Chiba 263-8522, Japan

<sup>2)</sup> Theory of Nanomaterials Group, KU Leuven, Celestijnenlaan 200F, B-3001 Leuven, Belgium

<sup>3)</sup> Department of Chemistry, National University of Singapore, Block S8 Level 3, 3 Science Drive 3, 117543, Singapore

<sup>4)</sup> NMR Research Unit, University of Oulu, P.O. Box 3000, FI-90014 Oulu, Finland

(Dated: 3 January 2025)

Broken-symmetry (BS) approaches are widely employed to evaluate Heisenberg exchange parameters, primarily in combination with DFT calculations. For many magnetic materials, BS-DFT calculations give reasonable estimations of exchange parameters although systematic failures have also been reported. While the latter were attributed to deficiencies of approximate exchange-correlation functional, we prove here by treating a simple model system that the broken-symmetry methodology has serious problems. Detailed analysis clarifies the intrinsic issue with the broken-symmetry treatment of low-spin states. It shows, in particular, that the error in the BS calculation of exchange parameter scales with the degree of covalency between the magnetic and the bridging orbitals. As a possible tool to overcome this intrinsic drawback of single-determinant BS approaches, we propose their extension to a minimal multiconfigurational version.

## I. INTRODUCTION

In the study of magnetism, understanding the exchange mechanisms and evaluating the exchange coupling parameters ( $J$ ) are of fundamental importance<sup>1-7</sup>. Current quantum chemistry methodologies offer approaches for evaluating the exchange parameters in various magnetic molecules and materials of experimental interest<sup>8-12</sup>. Among them, the broken-symmetry (BS) approach<sup>13-15</sup> has become a standard tool, especially for calculating  $J$  in large systems involving several magnetic centers. This method allows the extraction of the exchange coupling by relating the energies of high-spin and BS low-spin states to the corresponding spin configurations of the Heisenberg exchange model. This approach is universal and can be applied with various quantum chemistry methods, allowing for calculating the total energy of different electronic configurations. Most calculations of this type have been performed within density functional theory (DFT) and, to a much lesser extent, within Hartree-Fock approximation. Recently, calculations of exchange parameters with BS-coupled cluster (CC)<sup>16</sup>, BS- $G_0W_0$ <sup>17</sup>, and BS-self-consistent GW<sup>18,19</sup> method have also been reported.

Despite its simplicity, the BS-DFT approach provides reasonable exchange parameters, often close to experimental values, for many magnetic materials<sup>9,10,12,20</sup>. Simultaneously, many quantitative and qualitative failures have been reported and discussed<sup>21,22</sup>. In particular, the strong dependence of the calculated  $J$  on the exchange-correlation functionals in the DFT calculation was found<sup>22-27</sup>. Although the failures have often

been attributed to the limitations of quantum chemistry methods<sup>28</sup>, they may not be the sole reason.

Here, we prove the breakdown of the broken-symmetry approach for extracting  $J$  by applying it to a simple Hubbard model. We demonstrate that this breakdown originates from an artificial constraint on the multiconfigurational state imposed by the broken-symmetry determinant. The error becomes especially pronounced in the case of strong covalency between the magnetic centers and bridging ligands. To overcome this drawback, we propose a calculational scheme based on a minimal version of the multiconfigurational (MC) BS approach.

## II. EXACT VS BROKEN-SYMMETRY CALCULATIONS OF EXCHANGE PARAMETERS

To assess the performance of the BS method, we confront its prediction for the exchange parameter  $J$  with the results of exact diagonalization. To facilitate the subsequent analysis, we treated the simplest possible model that contains all the necessary physical ingredients.

### A. Generic three-site model

We consider a three-center system consisting of two half-filled magnetic orbitals (1,2) and one empty orbital ( $l$ ) at the bridging ligand group [see Fig. 1(a)]. While looking just as H-He-H on a minimal basis, such a model can describe real magnetic materials if proper orbitals 1, 2, and  $l$  are chosen<sup>33</sup>.

The model possesses inversion/reflection symmetry with respect to the ligand site and includes the nearest-neighbor electron transfer ( $t$ ) between the magnetic and the ligand orbital and the next-nearest neighbor electron transfer ( $t'$ ) between orbitals 1 and 2. Adding electron

<sup>a)</sup> Electronic mail: [naoya.iwahara@gmail.com](mailto:naoya.iwahara@gmail.com)

<sup>b)</sup> Electronic mail: [liviu.chibotaru@kuleuven.be](mailto:liviu.chibotaru@kuleuven.be)

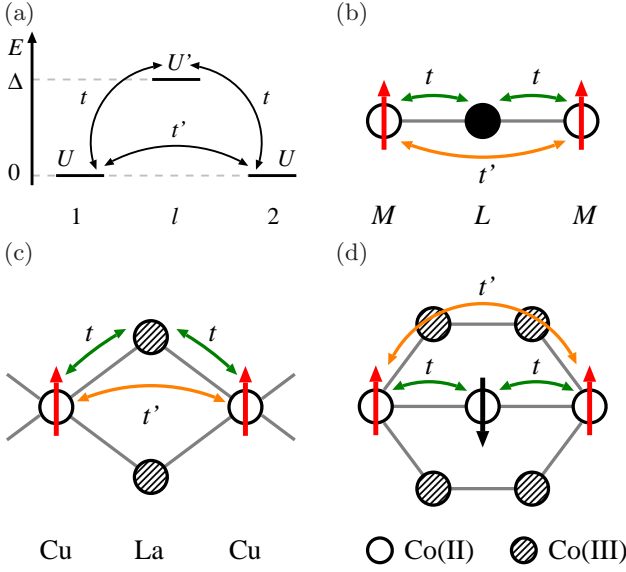


FIG. 1. Three-site systems. (a) Parametrization. The geometries of (b) trinuclear complex such as  $[\text{LFeCoFeL}]^{3+29}$ , (c) Cu chain<sup>30,31</sup>, and (d)  $\text{Co}_3^{\text{II}}\text{Co}_4^{\text{III}}$  complex<sup>32</sup>.

repulsion on sites, we end up with a  $t-t'$  Hubbard model:

$$\begin{aligned} \hat{H} = & \sum_{\sigma=\uparrow,\downarrow} t(\hat{a}_{1\sigma}^\dagger \hat{a}_{l\sigma} + \hat{a}_{l\sigma}^\dagger \hat{a}_{1\sigma} + \hat{a}_{2\sigma}^\dagger \hat{a}_{l\sigma} + \hat{a}_{l\sigma}^\dagger \hat{a}_{2\sigma}) \\ & + \sum_{\sigma=\uparrow,\downarrow} t'(\hat{a}_{1\sigma}^\dagger \hat{a}_{2\sigma} + \hat{a}_{2\sigma}^\dagger \hat{a}_{1\sigma}) + \sum_{\sigma=\uparrow,\downarrow} \Delta \hat{n}_{l\sigma} \\ & + U(\hat{n}_{1\uparrow} \hat{n}_{1\downarrow} + \hat{n}_{2\uparrow} \hat{n}_{2\downarrow}) + U' \hat{n}_{l\uparrow} \hat{n}_{l\downarrow}. \end{aligned} \quad (1)$$

Here,  $i$  indicates orbitals,  $\sigma$  is the electron spin projection,  $\hat{a}_{i\sigma}^\dagger$  and  $\hat{a}_{i\sigma}$  are electron creation and annihilation operators in the spin-orbital  $i\sigma$ , respectively;  $\hat{n}_{i\sigma} = \hat{a}_{i\sigma}^\dagger \hat{a}_{i\sigma}$ ,  $\Delta$  is the gap between metal and ligand orbital levels, and  $U$  and  $U'$  are the parameters of Coulomb repulsion in the magnetic and ligand orbitals, respectively. We assume the orthonormality of atomic orbitals,  $\langle i|j \rangle = \delta_{ij}$ . The sign of  $t$  does not influence the energy levels, hence, hereafter  $t \geq 0$ .

Despite the simplicity, this model reproduces all essential contributions to the exchange interaction between two unpaired spins except for the spin polarization of ligands. The inclusion of direct electron transfer ( $t'$ ) along with the intermediate one ( $t$ ) is indispensable for quantitative analysis of exchange interaction in many magnetic materials<sup>33</sup>. Besides conventional kinetic antiferromagnetic and potential ferromagnetic contributions<sup>1,34</sup>, it also allows us to identify the ferromagnetic kinetic exchange contribution<sup>35-39</sup>. The latter plays a vital role in complexes with strong metal-ligand covalency, such as the thiophenolate-bridged heterotrimeric complex  $[\text{LFeCoFeL}]^{3+29}$ , in which one orbital of the bridging ligand group containing the diamagnetic Co(III) is strongly hybridized with the magnetic orbitals at low-spin Fe(III) sites<sup>33,36,37</sup>. Such a generic situation [Fig. 1(b)] is met

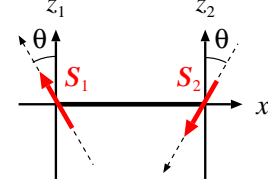


FIG. 2. Rotation of the spins for the magnetic force theorem calculations.

for numerous bridging groups L, the limitation to one empty or doubly occupied ligand orbital  $l$  being sufficient in many cases<sup>33</sup>. For the bridging geometry in Fig. 1(b),  $t'$  is expected to be significantly smaller than  $t$ . However, for strong metal-ligand covalency, the former can be far from negligible as in iron-sulfur bridged  $[\text{LFeCoFeL}]^{3+}$  where  $t' = 0.4|t|$ <sup>33</sup>. At the same time, we can easily conceive M-L-M structures where  $t'$  can be of similar magnitude with or even larger than  $t$  [Fig. 1(c),(d)]<sup>40</sup>.

Given the above arguments, a comparison of exact and BS calculations of  $J$  based on this model is expected to be conclusive in the quest for the validity of the latter. Moreover, the identification of the domain of parameters of Eq. (1) for which the discrepancy occurs will give a direct insight into the physical reasons for its breakdown<sup>41</sup>.

## B. Exact vs BS calculations of $J$

We calculate the exchange parameter of the model (1) within the full configuration interaction (CI) method, broken-symmetry Hartree-Fock (BS-HF) approximation, and the magnetic force theorem (MFT). In the first approach, we derive the exchange parameter  $J$  in the Heisenberg model,

$$\hat{H}_{\text{ex}} = J \hat{\mathbf{S}}_1 \cdot \hat{\mathbf{S}}_2, \quad (2)$$

by using the energy gap between the lowest high- and low-spin energy levels obtained. In this equation,  $\hat{\mathbf{S}}_i$  is a spin 1/2 operator on-site  $i = 1, 2$ . See for the details of the full CI Hamiltonian matrices Appendix A 1.

To estimate the exchange parameter for Eq. (2) by the BS-HF method, we use Yamaguchi's formula<sup>14</sup>:

$$J_{\text{BS}} = \frac{2(E_{\text{F}} - E_{\text{UHF}})}{\langle \hat{\mathbf{S}}^2 \rangle_{\text{F}} - \langle \hat{\mathbf{S}}^2 \rangle_{\text{UHF}}}, \quad (3)$$

where,  $\hat{\mathbf{S}} = \hat{\mathbf{S}}_1 + \hat{\mathbf{S}}_2$ ,  $\langle \hat{\mathbf{S}}^2 \rangle_{\text{F}} = 2$  and  $\langle \hat{\mathbf{S}}^2 \rangle_{\text{UHF}}$  is the expectation value of  $\hat{\mathbf{S}}^2$  for BS-HF wave function  $|\Psi_{\text{UHF}}\rangle$ . See for the detailed expressions for the BS-HF calculations Appendix A 2 b. When the BS state displays well-localized spin densities on sites, one can equally well use the Noodleman's expression for  $J_{\text{BS}}$ <sup>13</sup> because in this case,  $\langle \hat{\mathbf{S}}^2 \rangle_{\text{UHF}} \approx 1$ . However, the latter gradually deviates from unity with the change of  $t'$  and  $\Delta$  [see Appendix A 2 b]. Accordingly, the prediction based on Noodleman's

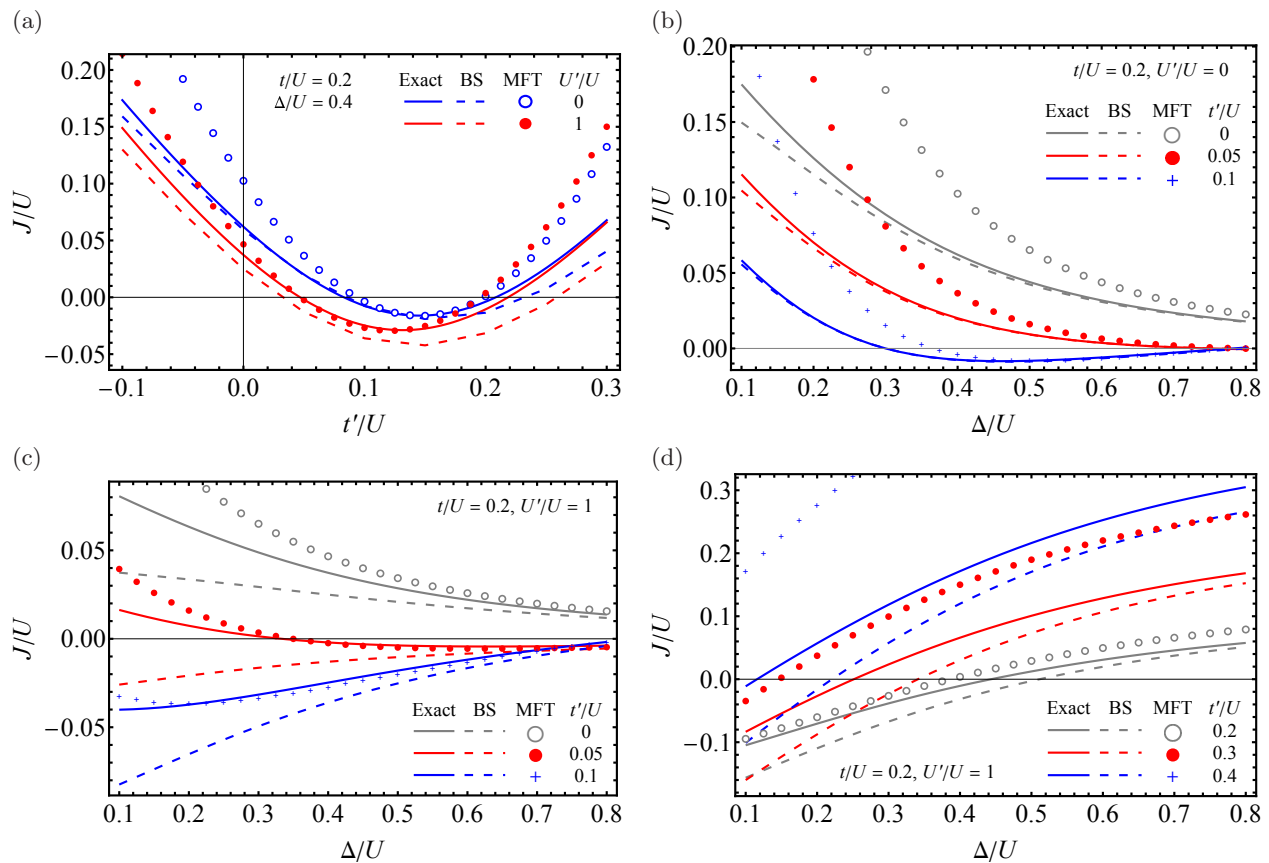


FIG. 3. Exact and approximate exchange parameters and the nature of the antiferromagnetic state.  $J$ ,  $J_{BS}$ , and  $J_{MFT}$  with respect to (a)  $t'/U$  and (b), (c), (d)  $\Delta/U$ . The parameters used for the simulations are written in the figure.

formula deviates from the result given by Eq. (3). In the limit of large M-L covalency, when the HF instability does not occur (the BS-HF determinant coincides with a restricted HF solution) so that  $\langle \hat{S}^2 \rangle_{\text{UHF}} = 0$ , the Noodleman's expression will be strongly in error while Eq. (3) still correct<sup>42</sup>.

We also calculate the exchange interaction using the magnetic force theorem<sup>43</sup>. In this approach, we compare the energy changes of the classical spin model and the BS-HF state by the rotations of the spins. Under the rotations of the antiparallel classical spins as in Fig. 2, the total energy is

$$E(\theta) = -J\mathbf{S}^2 \cos 2\theta \approx -J\mathbf{S}^2 (1 - 2\theta^2), \quad (4)$$

where  $\mathbf{S}$  is the classical spin vector, and the last expression assumes a small  $\theta$ . Within the quantum mechanical treatment, the rotation of the quantum spins of the BS-HF state is achieved by  $\hat{R}(\theta)|\Psi_{\text{UHF}}\rangle$  with

$$\hat{R}(\theta) = e^{i\hat{S}_{1y}\theta} e^{-i\hat{S}_{2y}\theta}. \quad (5)$$

By comparing the classical and quantum mechanical energies, we obtain  $J$ . See for the detailed expressions of the energy Appendix B.

Figure 3(a) shows the calculated exchange parameter in the function of  $t'/U$ . The exact  $J$  obtained from the

full CI calculations (solid), the broken-symmetry  $J_{BS}$  (dashed), and the magnetic force theorem  $J_{MFT}$  (symbols) exhibit similar behavior, whereas the approximate  $J$ 's are quantitatively and, under certain ranges of parameters, qualitatively different from the exact one.  $J_{BS}$  tends to overestimate the ferromagnetic contribution due to the contamination of the ferromagnetic component of about 40-50 % in the UHF energy (see Appendix A 2 b). The spin contamination in the BS-HF wave function makes the variational parameters (molecular orbital coefficients) not fully optimal for the description of the ground antiferromagnetic state<sup>44</sup>. Moreover, the number of the variational parameters for the BS-HF wave function is less than that for the exact solution, leading to a poor description of the antiferromagnetic state with the BS-HF wave function. For some range of  $t'/U$ , one can also see that  $J_{BS}$  qualitatively differs (opposite sign) from the exact  $J$ : Within  $0.03 \lesssim t'/U \lesssim 0.05$  and  $0.22 \lesssim t'/U \lesssim 0.26$  for  $U'/U = 1$  ( $0.21 \lesssim t'/U \lesssim 0.24$  for  $U'/U = 0$ ), the exact  $J$  becomes antiferromagnetic, whereas  $J_{BS}$  is ferromagnetic. The discrepancy is enlarged with the increase of the Coulomb repulsion on the bridging site,  $U'$ , implying that the mean-field description is not adequate. The static electron correlation effect is crucial to derive accurate  $J$ .

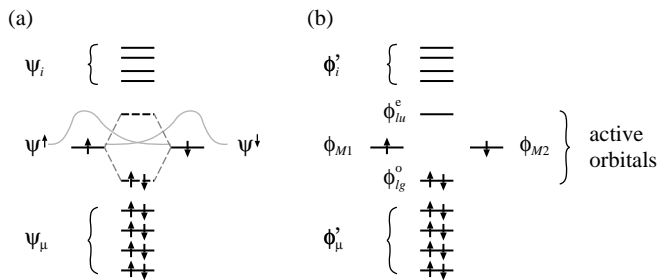


FIG. 4. (a) Partially restricted molecular orbitals and (b) active magnetic and ligand orbitals (solid lines).

We can see the importance of the electron correlation for the description of  $J$  by modulating the covalency via  $\Delta$ . From a detailed analysis of the present model, we have demonstrated that the static electron correlation effect is enhanced for small  $\Delta$ <sup>33</sup>. Figures 3(b), (c) show that  $J_{\text{BS}}$  deviates from exact  $J$  when  $\Delta$  lowers and the covalency effect enhances: The discrepancy is further enhanced by turning on  $U'$ .

$J_{\text{MFT}}$  shows opposite tendency to  $J_{\text{BS}}$ . First,  $J_{\text{MFT}}$  overestimates the antiferromagnetic contribution [Fig. 3(a)]:  $J_{\text{MFT}}$  is ferromagnetic in a smaller range of  $t'/U$  than the exact  $J$  does and exhibits larger antiferromagnetic contribution. Second, the description of  $J_{\text{MFT}}$  becomes poor when the covalency effect becomes stronger by reducing  $U'$  or increasing  $t$ 's [Figs. 3(b)-(d)]. Since the magnetic force theorem calculations assume well-localized classical spins, this method would not work well when the covalency effects are strong.

The present analysis shows that the BS approach and the MFT one fail when the magnetic electrons are delocalized over the bridging ligand, realized at sufficiently small  $\Delta$ . Small values of  $\Delta$  are not unusual when the metal and ligand orbitals are close to resonance, e.g., in iron-sulfur complexes<sup>45</sup>. Also, as emphasized above, finite and even large  $t'$  is not surprising in real materials.

The breakdown of the BS approach for the calculation of  $J$  ultimately originates from the lack of sufficient flexibility of the BS-HF determinant. Indeed, while CI and HF wave functions for ferromagnetic states coincide in our model, they differ for the antiferromagnetic states through fewer variational parameters in the BS-HF treatment (see Appendix A 2 b). The absence of approximation in the derivation of exact states excludes any doubts that the discrepancy shown by the BS approach is only due to the intrinsic drawback of the latter. In particular, the significance of adequate treatment of electron correlation in the antiferromagnetic states is revealed. To eliminate this intrinsic drawback, the BS approach should be extended as suggested below.

### III. EXTENSION OF THE BS APPROACH FOR THE EXCHANGE PARAMETERS

A reliable multiconfigurational calculation of exchange parameters based on Hartree-Fock orbitals as e.g., within the CASSCF/CASPT2 approximation<sup>46</sup>, poses difficulties, especially, for large molecules. The main drawback of this approach is an insufficient account of dynamical correlation resulting in underestimation of the intersite electron transfer and overestimation of on-site electron repulsion. On the contrary, the dynamical correlation is intrinsically contained in DFT, CC and GW, which is the reason why the BS approaches became a standard tool for the calculation of  $J$ . Here we suggest an extension of this approach in order to cure its intrinsic drawbacks described above. To this end, we propose a minimal multiconfigurational version involving electronic configurations built on several active orbitals derived from a preliminary BS calculation. To exemplify this methodology, we consider the simplest case of two unpaired electrons in equivalent magnetic (metal) sites, the extension to other situations being straightforward.

#### A. Spin polarization contribution

After a standard BS calculation, a partly restricted calculation is performed in which the two magnetic orbitals containing unpaired electrons ( $\psi^\sigma$ ) remain unchanged, while the doubly occupied and empty orbitals are reoptimized under spin restriction [Fig. 4(a)]. All molecular orbitals are orthogonal to each other except for the magnetic ones:

$$\langle \psi^\uparrow | \psi^\downarrow \rangle = S_M. \quad (6)$$

The difference between total energies obtained from BS and partly restricted calculation for the HS and BS states gives the spin polarization contribution to the energy of the latter. Accordingly, the spin polarization contribution to the exchange parameter is given by

$$J_{\text{pol}} = J_{\text{BS}} - J_{\text{res}}, \quad (7)$$

where  $J_{\text{BS}}$  is calculated as in Eq. (3) and  $J_{\text{res}}$  is calculated as follows:

$$J_{\text{res}} = \frac{2(E_{\text{HS}}^{\text{res}} - E_{\text{BS}}^{\text{res}})}{1 + S_M^2}. \quad (8)$$

This equation is a particular case of the Yamaguchi's formula (3) when the spin contamination comes from a single pair of non-orthogonal magnetic orbitals<sup>47</sup>. The total exchange parameter consists of the contributions described in the previous section ( $J$ ) and the spin-polarization contribution (7):

$$J_{\text{tot}} = J + J_{\text{pol}}. \quad (9)$$

Note that the inherent error of the BS approach is expected to be almost canceled in  $J_{\text{pol}}$  because the energy of the BS configuration enters both terms in Eq. (7).

## B. The active orbitals

To overcome the drawbacks of the BS approach, we should be in line with the results of the previous section, i.e. identify a set of effective magnetic and bridging ligand orbitals (active orbitals) and undertake a multi-configurational calculation on their basis. Then from the energies of the lowest  $S = 0$  and  $S = 1$  states the parameter  $J$  is extracted. Following the previous section, these active orbitals are chosen in a form which allows the expansion of the BS magnetic orbitals  $\psi^\sigma$  solely in their basis. The construction of these active orbitals is shown below for a simplest system of two equivalent magnetic (metal) sites  $i=1,2$  with one unpaired electron,  $S_i=1/2$ . Furthermore the complex is supposed to possess a mirror symmetry under which the BS orbitals  $\psi^\sigma$  pass into each other,  $\sigma_h \psi^\uparrow = \psi^\downarrow$  [Fig. 4(a)], whereas the restricted molecular orbitals  $\{\psi_i, \psi_\mu\}$  are either even or odd with respect to this transformation, i.e., are characterized by indices  $g$  and  $u$  respectively<sup>48</sup>.

For this symmetric complex the orbitals  $\psi^\sigma$  are decomposed into four active orbitals (see Appendix C):

$$\begin{aligned}\psi^\uparrow &= c_1 \phi_{M_1} + c_2 \phi_{M_2} + c_g^o \phi_{lg}^o + c_u^e \phi_{lu}^e, \\ \psi^\downarrow &= c_2 \phi_{M_1} + c_1 \phi_{M_2} + c_g^o \phi_{lg}^o - c_u^e \phi_{lu}^e,\end{aligned}\quad (10)$$

where  $\phi_{M_1}$  and  $\phi_{M_2}$  are magnetic orbitals centered at the metal sites 1 and 2, respectively, accommodating unpaired magnetic electrons in the ground electronic configuration [Fig. 4(b)].  $\phi_{lg}^o$  and  $\phi_{lu}^e$  are effective bridging ligand orbitals,

$$\phi_{lg}^o = b_g^o \psi_{lg}^o + d_g^o \psi_g, \quad \phi_{lu}^e = b_u^e \psi_{lu}^e + d_u^e \psi_u, \quad (11)$$

where  $\psi_{lg}^o$  and  $\psi_{lu}^e$  are linear combinations of doubly occupied and empty restricted molecular orbitals, respectively [see Fig. 4(a)]:

$$\psi_{lg}^o = \sum_\mu a_{\mu g} \psi_{\mu g}, \quad \psi_{lu}^e = \sum_i a_{iu} \psi_{iu}, \quad (12)$$

while  $\psi_{g,u}$  are symmetrized combinations of  $\psi^\sigma$ ,

$$\psi_{g,u} = \frac{1}{2(1 \pm S_M)} (\psi^\uparrow \pm \psi^\downarrow). \quad (13)$$

One should note that the four orbitals entering the r.h.s. of Eq. (11) are automatically orthogonal, so that the normality of  $\phi_{lg}^o$  and  $\phi_{lu}^e$  imposes conventional relations for the expansion coefficients. The orthogonality between the orbitals Eqs. (10) and (11) gives (see Appendix C):

$$c_g^o = \frac{d_g^o}{\sqrt{2(1 + S_M)}}, \quad c_u^e = \frac{d_u^e}{\sqrt{2(1 - S_M)}}, \quad (14)$$

whereas from the normality of  $\psi^\sigma$  and orthogonality of  $\phi_{M_1}$  and  $\phi_{M_2}$  we extract the coefficients  $c_1$  and  $c_2$ , Eq. (C3), entering the decomposition (10). As Eqs. (14) and (C3) show, all coefficients in this decomposition are

expressed via  $d_g^o$  and  $d_u^e$ , which together with the coefficients  $\{a_{\mu g}\}$  and  $\{a_{iu}\}$  are the variational parameters defining the two active ligand orbitals in Eq. (11). Once these are found from an optimization procedure specified below, all expansion coefficients in Eqs. (10) can be calculated, which allows via the knowledge of  $\psi^\sigma$  to determine straightforwardly from these equations for the active magnetic orbitals  $\phi_{M_1}$  and  $\phi_{M_2}$  [Eq. (C4)].

In the case of non-equivalent magnetic centers, the two BS magnetic orbitals  $\psi^\sigma$  will not be related by symmetry anymore. Therefore, there is no reason to expect that they will decompose through common active ligand orbitals as in Eq. (10) but rather through different ones. Passing from two different active ligand orbitals of each type to their orthogonal combinations, we can decompose  $\psi^\uparrow$  and  $\psi^\downarrow$  into six common active orbitals: two magnetic, two ligand of doubly occupied type and two ligand of empty type. This scheme is straightforwardly generalized to several unpaired electrons on magnetic sites and more than two magnetic centers. In the absence of symmetry we will have to define for each magnetic electron ( $n$ ) one magnetic ( $\phi_{M_n}$ ) and two ligand ( $\phi_{ln}^o$  and  $\phi_{ln}^e$ ) active orbitals. The latter are written in analogy to Eq. (11) as follows:

$$\begin{aligned}\phi_{ln}^o &= \sum_m (b_{nm}^o \psi_{lm}^o + d_{nm}^o \psi_m), \\ \phi_{ln}^e &= \sum_m (b_{nm}^e \psi_{lm}^e + d_{nm}^e \psi_m),\end{aligned}\quad (15)$$

where  $\psi_{lm}^{\circ,e}$  are suitable combinations of occupied and empty restricted orbitals,

$$\psi_{lm}^o = \sum_\mu a_{m\mu}^o \psi_\mu, \quad \psi_{lm}^e = \sum_i a_{mi}^e \psi_i, \quad (16)$$

and  $\psi_m$  are arbitrary orthogonal combinations of BS magnetic orbitals  $\{\psi_m^{\text{BS}}\}$ . The indices  $n$  and  $m$  in Eq. (15) run over the total number  $N_m$  of BS magnetic orbitals (usually coinciding with the number of magnetic electrons). With knowledge of active ligand orbitals (15), the active magnetic orbitals  $\phi_{M_n}$  are derived from the relations [cf. Eq. (10)]

$$\psi_n = \sum_m (c_{nm} \phi_{M_m} + c_{nm}^o \phi_{lm}^o + c_{nm}^e \phi_{lm}^e) \quad (17)$$

for a given set of expansion coefficients  $\{c_{nm}, c_{nm}^o, c_{nm}^e\}$ .

Besides serving as a tool to calculate  $J$ , this methodology allows to extract the magnetic and effective ligand orbitals in a strict variational way. The existent approaches merely identify them with some Wannier orbitals constructed from arbitrarily chosen group of molecular/band orbitals<sup>49</sup>, an a priori unjustifiable and often unreliable procedure, especially, for large ligands.

## C. A minimal version of MC extension

Once the active magnetic and bridging ligand orbitals are defined, the lowest spin states are obtained as com-



binations of the corresponding electronic configurations  $\Phi_I$ :

$$\Psi = \sum_I C_I \Phi_I, \quad (18)$$

where  $C_I$  are variational parameters found from a multiconfigurational calculation. Another set of variational parameters are the expansion coefficients of the active magnetic and ligand orbitals, Eqs. (15)-(17).

The main difference from other versions of MC calculations is that now one should apply this treatment not to a group of canonical restricted orbitals, such as  $\psi_\mu$  and  $\psi_i$  in Fig. 4, but to their linear combinations ( $\phi_{ln}^o$ ,  $\phi_{ln}^e$ ,  $\phi_{Mn}$ ) which are not eigenfunctions of the corresponding mean-field, e.g., Kohn-Sham (KS) operator. This implies orthogonalization of all other doubly occupied restricted orbitals to the active ligand orbitals (15) or, equivalently, to the orbitals (16), i.e. construction of their orthogonal linear combinations  $\{\psi'_\mu\}$  and  $\{\psi'_i\}$ , respectively [Fig. 4(b)]. In practice, the knowledge of the form of the latter (coefficients of their decomposition in terms of original  $\{\psi_\mu\}$  and  $\{\psi_i\}$ ) is not needed. The reason is the known invariance of the electronic configurations under arbitrary unitary transformations in the space of fully occupied (or fully empty) orbitals<sup>50</sup>, which underlies the following equality of determinants:

$$\begin{aligned} & |\psi_{l1}^o \bar{\psi}_{l1}^o \cdots \psi_{lN_m}^o \bar{\psi}_{lN_m}^o \psi'_{N_m+1} \bar{\psi}'_{N_m+1} \cdots \psi'_\mu \bar{\psi}'_\mu \cdots \psi'_{N_d} \bar{\psi}'_{N_d}| \\ &= |\psi_1 \bar{\psi}_1 \cdots \psi_\mu \bar{\psi}_\mu \cdots \psi_{N_d} \bar{\psi}_{N_d}|, \end{aligned} \quad (19)$$

where  $N_d$  is the number of doubly occupied restricted orbitals in the DFT calculation. Since all configurations  $\Phi_I$  in Eq. (18) involve either the l.h.s. determinant as is or with few electrons removed from a relatively small number of orbitals  $\psi_{ln}^o$ ,  $\bar{\psi}_{ln}^o$ , we can describe them via few holes added to the core determinant (19). Since in addition we are not re-optimizing the orbitals  $\psi_\mu$  during the MC calculation, the determinant in the r.h.s. represents a ‘‘vacuum function’’ for the added holes. At the same time the occupation of BS orbitals (their combinations  $\psi_m^{\text{BS}}$ ) and empty restricted orbitals  $\psi_i$  is described in the electronic representation. In this way the wave functions  $\Phi_I$  in the expansion (18) involve explicitly only few electrons in the orthogonal BS orbitals and empty restricted orbitals and few holes in the doubly occupied restricted orbitals. Details of such electron-hole description are given in Appendix C 2.

Having established the rules for constructing the electronic configurations  $\Phi_I$  in the mixed electron-hole representation, the calculation of the matrix elements  $H_{IJ}$  of the corresponding Hamiltonian (C10) can be done straightforwardly. Within an explicit version of MC BS calculation one should minimize the functional:

$$E = \sum_{I,J} C_I^* C_J H_{IJ} (\{a_{m\mu}^o, a_{mi}^e, b_{nm}^{o,e}, d_{nm}^{o,e}, c_{nm}, c_{nm}^{o,e}\}), \quad (20)$$

with respect to the CI and orbital coefficients (subject to corresponding orthonormal conditions) in full analogy to a CASSCF calculation<sup>51</sup>.

In this work we do not discuss the implementation of the proposed approach. One should mention, however, that the feasibility of this scheme depends on the evaluation of off-diagonal matrix elements in Eq. (20). It is a quite straightforward procedure for HF, CC and even GW approaches. As for DFT, the evaluation of  $H_{IJ}$  can only be done indirectly, within an uncontrolled approximation. Given the popularity of DFT calculations, we review below the MC DFT approaches used to date.

## 1. MC DFT approaches

Several approaches to the MC DFT have been developed in the past. These include re-definition of Kohn–Sham (KS) theory to include multiconfigurational reference wave function from the start<sup>52,53</sup>, a range-separation of the electron–electron interaction into a short-range part described by a local correlation potential and a long-range part described by the correlation arising from the MC expansion<sup>54–56</sup>, a method based on a local scaling factor of the DFT correlation energy<sup>57</sup> and more complicated methods for the balanced treatment of MC and DFT correlation effects<sup>58</sup>, as well as methods based on a correlation separation using the LDA correlation energy density<sup>59–61</sup>. As a less rigorous approach, a reparametrization of the XC functional in the context of an MC expansion<sup>62,63</sup> and the rescaling of the matrix elements of the CI matrix constructed in the presence of the XC potential by empirical coefficients<sup>64</sup> have been proposed. Another actively developed approach is the so-called ensemble-referenced Kohn–Sham (REKS) method<sup>65–67</sup>, in which the variational entity is an ensemble density expanded as a linear combination of densities corresponding to individual determinants. We note that all these approaches can be applied for our problem in a slightly modified form.

Concerning Eq. (20), within DFT the matrix elements are supposed to be rescaled by empirical coefficients<sup>64</sup>. This approach is closely related to the actively used nowadays ROCIS method, a single-configuration multireference approach for evaluation of electronic excitation of inner shells<sup>68,69</sup>, which also employs the rescaling of CI matrix elements using empirical factors. As starting point in the self-consistent calculation, we identify  $\phi_{Mn}^e$  with  $\psi_n$  which are maximally close to the original  $\psi_m^{\text{BS}}$ , obtained from the latter via e.g. a Löwdin orthogonalization ( $c_{nm} = \delta_{nm}$ ,  $c_{nm}^{o,e} = 0$ ); the orbitals  $\phi_{ln}^{o,e}$  are identified with corresponding restricted orbitals having maximal weight in the pairs of neighbor (overlapping)  $\psi_m^{\text{BS}}$ .

Another approach, the so-called CAS-DFT<sup>70</sup>, considers the functional

$$E = F^{\text{CAS-DFT}}[\Psi] + E_C^{\text{CAS-DFT}}[\rho, P], \quad (21)$$

where the first term is the CAS energy (20) in its conventional form (without rescaling), while the second term is the correlation energy in which the conventional spin densities are replaced by combinations of total CAS density  $\rho(\mathbf{r})$  and on-top pair density  $P(\mathbf{r}, \mathbf{r})$ <sup>71</sup>. As appropriate  $E_C^C$ , a Colle-Salvetti<sup>72,73</sup> or Lee-Yang-Parr<sup>74</sup> correlation functional should be used. In order to avoid a double counting of dynamical correlation energy covered by the first term of (21),  $E_C^{\text{CAS-DFT}}[\rho, P]$  is evaluated with local rescaling factors<sup>70</sup>. This rescaling can be neglected when a few configurations are mixed in the CASSCF wave function, which is certainly the case here. Indeed, given the relative weakness of the exchange coupling in most magnetic complexes, we will only need to consider singly and doubly excited configurations from reference one(s) resulting in their limited amount even for a large space of active magnetic and ligand orbitals.

A related version of CAS-DFT is the actively developed multiconfigurational pair-density functional theory (MC-PDFT)<sup>75,76</sup>. It is currently implemented in OpenMolcas<sup>77</sup> with a plethora of on-top functionals, corresponding to translated exchange-correlation functionals, and different versions of MC calculations. It has been successfully applied to the calculation of relative energy levels in exchange-coupled systems<sup>78</sup>, the calculation of singlet-triplet splittings in main-group and organic systems<sup>79-81</sup> and the relative spin-state energetics of coordinated metal ions<sup>82,83</sup>.

Contrary to these methods which do not involve the KS density, the REKS functional is a linear combination KS energies corresponding to different electronic configurations of active electrons. The coefficients of this combination are expressed via the fractional occupation numbers in the total REKS density through model considerations<sup>65-67</sup>. The weak point of this approach is that it is designed for very small active spaces and cannot be easily extended over, e.g., CAS(4,4). Note that the latter will be already sufficient for the calculation of exchange parameters in symmetric dimers with one unpaired electron per site, for which the expressions derived in Sec. III B and Appendix C can be applied directly. The densities corresponding to different electronic configurations of active electrons are calculated as described in Appendix C 2. As an example, Eq. (C8) gives the total density for the ground configuration  $\Phi_1$ . One should have in mind that the self-consistent procedure involves variation of orbital coefficients defining the active orbitals only. The same refers also to other approaches mentioned above.

One should note that the MC DFT approaches have been straightforwardly applied to the calculation of exchange parameters in organic materials<sup>61,84</sup> and complexes (an overview of earlier work can be found in Ref. 85). They generally produced results comparable in accuracy with BS DFT calculations. Thus CASSCF(2,2) calculations of magnetic coupling in Cu(II) binuclear complexes by the REKS method have shown that imposing strict spin symmetry does not improve the BS DFT eval-

uation of exchange parameters<sup>86</sup>. While the active space in these calculations was restricted to magnetic orbitals only, we stress that including specially designed active ligand orbitals are expected to improve the predictability of  $J$  in such calculations, as they would certainly improve the BS DFT results according to the present study.

## IV. CONCLUSION

In this work, we prove the breakdown of the broken-symmetry approach for the evaluation of exchange parameters by applying it to a generic three-site model. We show that this breakdown originates from an artificial constraint on multiconfigurational state imposed by the broken-symmetry determinant. The error becomes especially pronounced in the case of strong covalency between magnetic centers and the bridging ligand. To cure this drawback, we propose a calculational scheme based on a minimal multiconfigurational extension of the BS approach. An example of such an economical employment of the CI space for the description of realistic systems is the recently developed GS-ROCIS method<sup>87</sup>.

As active orbitals in the MC calculations, the proposed method employs effective magnetic and bridging ligand type orbitals, whose construction and self-consistent determination is outlined in detail. This approach can be used with any a variety of quantum chemistry software involving MC and BS calculations, in particular, with any version of existent MC DFT code, the only required modification being the implementation of optimization of the coefficients defining the active orbitals. Besides possible improvement in the prediction of exchange parameters, we expect this approach to help resolving the issue related to the strong variation of the performance of a given exchange-correlation functional for evaluation of  $J$  in different magnetic systems<sup>21,22</sup>, which variability seems to be less pronounced for other molecular properties calculated with DFT.

## ACKNOWLEDGEMENT

N.I. was supported by Grant-in-Aid for Scientific Research (Grant No. 22K03507) from the Japan Society for the Promotion of Science, and Chiba University Open Recruitment for International Exchange Program. Z.H. was supported by the China Scholarship Council, and the financial support of research projects A-8000709-00-00, A-8000017-00-00, and A-8001894-00-00 of the National University of Singapore. A.M. A. M. acknowledges funding provided by the Research Council of Finland (grant no. 362649).

## AUTHOR DECLARATIONS

### Conflict of Interest

The authors have no conflicts to disclose.

### Author Contributions

N. Iwahara: Conceptualization (equal); Formal analysis (lead); Investigation (equal); Writing – original draft (equal); Writing – review & editing (equal). Z. Huang: Writing – review & editing (equal). A. Mansikkamäki: Writing – review & editing (equal). L. F. Chibotaru: Conceptualization (equal); Project administration (lead); Investigation (equal); Writing – original draft (equal); Writing – review & editing (equal).

### DATA AVAILABILITY

The data that support the findings of this study are available from the corresponding authors upon request.

### Appendix A: Solutions for the generic three-site model

The full CI and broken-symmetry HF treatment of the Hubbard model (1) is shown below.

#### 1. Exact solutions

##### a. Ferromagnetic state

The basis for the ferromagnetic (spin triplet,  $S = 1$ ) states  $|F, M_S; n, p\rangle$  are

$$|F, 1; 0-\rangle = |12\rangle, \quad |F, 1; 1\mp\rangle = \frac{1}{\sqrt{2}}(|1l\rangle \pm |l2\rangle) \quad (\text{A1})$$

and

$$\begin{aligned} |F, 0; 0-\rangle &= \frac{1}{\sqrt{2}}(|1\bar{2}\rangle - |2\bar{1}\rangle), \\ |F, 0; 1\mp\rangle &= \frac{1}{2}(|1\bar{l}\rangle - |l\bar{1}\rangle \pm |l\bar{2}\rangle \mp |2\bar{l}\rangle), \end{aligned} \quad (\text{A2})$$

respectively. Here,  $|ij\rangle$  and  $|i\bar{j}\rangle$  etc. indicate Slater determinants, spin up and down are specified by without and with bar, “F” stands for ferromagnetic state,  $M_S$  the  $z$  component of total spin,  $n$  distinguishes the  $S, M_S$  states,  $p$  ( $= \pm$ ) the parity of the spatial part (symmetric or antisymmetric). The Hamiltonian matrix is written as

$$\mathbf{H}_F = \begin{pmatrix} 0 & \sqrt{2}t & 0 \\ \sqrt{2}t & \Delta - t' & 0 \\ 0 & 0 & \Delta + t' \end{pmatrix}, \quad (\text{A3})$$

The order of the basis is  $|0-\rangle, |1-\rangle, |1+\rangle$  (“F” and  $M_S$  are omitted). The ground energy is obtained from the  $2 \times 2$  block, and the ground state is expressed as

$$|\Psi_{M_S}^F\rangle = \sum_{i=0,1} |F, M_S; i-\rangle C_i. \quad (\text{A4})$$

##### b. Antiferromagnetic state

The symmetrized antiferromagnetic (singlet) states  $|\text{AF}; n, p\rangle$  are

$$\begin{aligned} |\text{AF}; 0+\rangle &= \frac{1}{\sqrt{2}}(|1\bar{2}\rangle + |2\bar{1}\rangle), \\ |\text{AF}; 1\pm\rangle &= \frac{1}{2}(|1\bar{l}\rangle + |l\bar{1}\rangle \pm |l\bar{2}\rangle \pm |2\bar{l}\rangle), \\ |\text{AF}; 2\pm\rangle &= \frac{1}{\sqrt{2}}(|1\bar{1}\rangle \pm |2\bar{2}\rangle), \\ |\text{AF}; 3+\rangle &= |\bar{l}\bar{l}\rangle. \end{aligned} \quad (\text{A5})$$

The Hamiltonian matrix is written as

$$\mathbf{H}_{\text{AF}} = \begin{pmatrix} 0 & \sqrt{2}t & 2t' & 0 & 0 & 0 \\ \sqrt{2}t & \Delta + t' & \sqrt{2}t & 2t & 0 & 0 \\ 2t' & \sqrt{2}t & U & 0 & 0 & 0 \\ 0 & 2t & 0 & 2\Delta + U' & 0 & 0 \\ 0 & 0 & 0 & 0 & \Delta - t' & \sqrt{2}t \\ 0 & 0 & 0 & 0 & \sqrt{2}t & U \end{pmatrix}, \quad (\text{A6})$$

in the order of the basis  $|0+\rangle, |1+\rangle, |2+\rangle, |3+\rangle, |1-\rangle, |2-\rangle$  (“AF” is omitted). The ground energy is obtained from the spatially symmetric part (the  $4 \times 4$  block), and the ground antiferromagnetic state is written as

$$|\Psi^{\text{AF}}\rangle = \sum_{i=0}^3 |\text{AF}; i+\rangle C_i. \quad (\text{A7})$$

In Fig. 2 in the main text, the weight of each configuration  $w_i = C_i^2$  in function of  $\Delta/t$  is displayed.

#### 2. Hartree-Fock solutions

##### a. Ferromagnetic state

From the atomic orbitals,  $|1\rangle, |2\rangle$ , and  $|l\rangle$ , two symmetric (S) and one antisymmetric (A) molecular orbitals are constructed:

$$\begin{aligned} |\psi_S\rangle &= \frac{A}{\sqrt{2}}(|1\rangle + |2\rangle) + B|l\rangle, \\ |\psi'_S\rangle &= \frac{B}{\sqrt{2}}(|1\rangle + |2\rangle) - A|l\rangle, \\ |\psi_A\rangle &= \frac{1}{\sqrt{2}}(|1\rangle - |2\rangle). \end{aligned} \quad (\text{A8})$$



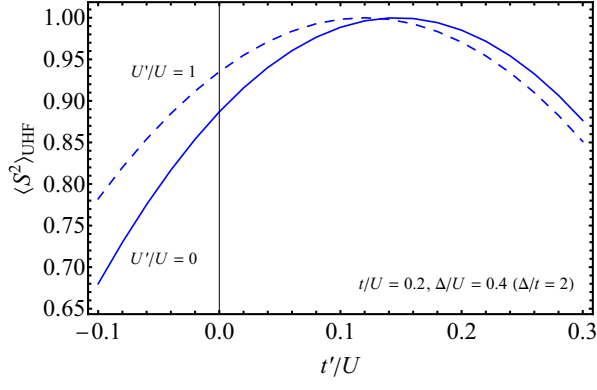


FIG. 5.  $\langle S^2 \rangle_{\text{UHF}}$  with respect to  $t'/U$ . The same parameters as Fig. 3(a) are used.

The coefficients  $A$  and  $B$  are real, and the molecular orbitals are normalized. The high-spin state with maximal projection  $M_S = 1$ ,

$$|\Psi_{\text{HF}}^{\text{F}}\rangle = |\psi_{\text{S}}\psi_{\text{A}}\rangle = -A|F, 1; 0-\rangle - B|F, 1; 1-\rangle. \quad (\text{A9})$$

Since both the high-spin full CI and HF wave functions contain one variational parameter, the exact high-spin state can be obtained by HF approach.

### b. Unrestricted low-spin state

The molecular orbitals used for the unrestricted HF (UHF) method are written as

$$\begin{aligned} |\psi^\uparrow\rangle &= C_1|1\rangle + C_2|2\rangle + C_l|l\rangle, \\ |\psi^\downarrow\rangle &= C_2|1\rangle + C_1|2\rangle + C_l|l\rangle, \end{aligned} \quad (\text{A10})$$

where the coefficients  $C_1, C_2, C_l$  are real and the molecular orbitals are normalized. The low-spin UHF wave function,

$$\begin{aligned} |\Psi_{\text{UHF}}\rangle &= |\psi^\uparrow\bar{\psi}^\downarrow\rangle \\ &= \frac{C_1^2 + C_2^2}{\sqrt{2}}|\text{AF}; 0+\rangle + (C_1 + C_2)C_l|\text{AF}; 1+\rangle \\ &\quad + \sqrt{2}C_1C_2|\text{AF}; 2+\rangle + C_l^2|\text{AF}; 3+\rangle \\ &\quad + \frac{C_1^2 - C_2^2}{\sqrt{2}}|\text{F}; 0; 0-\rangle + (C_1 - C_2)C_l|\text{F}; 0; 1-\rangle. \end{aligned} \quad (\text{A11})$$

This expression shows both the ferro- and antiferromagnetic configurations are included in  $|\Psi_{\text{UHF}}\rangle$ . Note that the exact low-spin states are expressed by three parameters, while there are only two parameters in the UHF states. Based on the wave function (A11), the UHF energy and  $\langle \hat{S}^2 \rangle_{\text{UHF}}$  are calculated as, respectively,

$$E_{\text{UHF}} = 4tC_l(C_1 + C_2) + 4t'C_1C_2 + 2\Delta C_l^2 + 2UC_1^2C_2^2 + U'C_l^4, \quad (\text{A12})$$

$$\langle \hat{S}^2 \rangle_{\text{UHF}} = \langle \hat{S}^2 \rangle_{\text{F}} \left[ \frac{(C_1^2 - C_2^2)^2}{2} + (C_1 - C_2)^2 C_l^2 \right] \quad (\text{A13})$$

Calculated  $\langle \hat{S}^2 \rangle_{\text{UHF}}$  is shown in Fig. 5.

### c. Spin symmetry adapted state

We define the AF part of the AF part of UHF wave function as the spin symmetry adapted (SA) HF wave function:

$$|\Psi_{\text{SAHF}}\rangle = \frac{1}{\sqrt{2(1 + S_M^2)}} (|\psi^\uparrow\bar{\psi}^\downarrow\rangle + |\psi^\downarrow\bar{\psi}^\uparrow\rangle) \quad (\text{A14})$$

where  $S_M = 2C_1C_2 + C_l^2$  is the overlap between  $\psi^\uparrow$  and  $\psi^\downarrow$  (A10). The energy for the SA-HF state is

$$\begin{aligned} E_{\text{SAHF}} &= \frac{1}{1 + S_M^2} \left[ 4t(1 + S_M)(C_1 + C_2)C_l \right. \\ &\quad \left. + t'(4C_1C_2 + 2(C_1^2 + C_2^2)S_M) \right. \\ &\quad \left. + 2\Delta C_l^2(1 + S_M) + 4UC_1^2C_2^2 + 2U'C_l^4 \right] \quad (\text{A15}) \end{aligned}$$

$J$  was calculated using a modified Yamaguchi's formula in which  $E_{\text{UHF}}$  and  $\langle S^2 \rangle_{\text{UHF}}$  are replaced by  $E_{\text{SA}}$  and  $\langle S^2 \rangle_{\text{SA}} = 0$ , respectively.

## Appendix B: Expressions for the magnetic force theorem

Here, we show the detailed expressions used for the magnetic force theorem calculations of  $J$ . The rotations of the quantum spins of the broken symmetry state results in

$$\begin{aligned} \hat{R}(\theta)|\psi^\uparrow\bar{\psi}^\downarrow\rangle &= \cos^2 \frac{\theta}{2} |\psi^\uparrow\bar{\psi}^\downarrow\rangle - \sin^2 \frac{\theta}{2} |\psi^\downarrow\bar{\psi}^\uparrow\rangle \\ &\quad - \frac{1}{2} \sin \theta (|\psi^\uparrow\psi^\downarrow\rangle + |\bar{\psi}^\uparrow\bar{\psi}^\downarrow\rangle). \end{aligned} \quad (\text{B1})$$

In terms of the configurations, we have

$$\begin{aligned} \hat{R}(\theta)|\psi^\uparrow\bar{\psi}^\downarrow\rangle &= \cos \theta |\psi^\uparrow\bar{\psi}^\downarrow\rangle - \sum_{M_S=\mp 1} \frac{1}{2} \sin \theta [(C_1^2 - C_2^2) \\ &\quad \times |F, M_S; 0\rangle + \sqrt{2}(C_1 - C_2)C_l|F, M_S; 1-\rangle]. \end{aligned} \quad (\text{B2})$$

The energy expectation value for  $\hat{R}(\theta)|\psi^\uparrow\bar{\psi}^\downarrow\rangle$  is

$$\begin{aligned} E(\theta) &\approx E_{\text{UHF}} + \theta^2 [-4(C_1 + C_2)C_l(2C_1C_2 + C_l^2)t \\ &\quad - 2(C_1^2 + C_2^2)(2C_1C_2 + C_l^2)t' \\ &\quad - 2(C_1C_2 + C_l^2)C_l^2\Delta - 2C_1^2C_2^2U - C_l^4U']. \end{aligned} \quad (\text{B3})$$

Comparing Eqs. (4) and (B3), we obtain

$$\begin{aligned} J_{\text{MFT}} &= 2 [-4(C_1 + C_2)C_l(2C_1C_2 + C_l^2)t \\ &\quad - 2(C_1^2 + C_2^2)(2C_1C_2 + C_l^2)t' \\ &\quad - 2(C_1C_2 + C_l^2)C_l^2\Delta - 2C_1^2C_2^2U - C_l^4U']. \end{aligned} \quad (\text{B4})$$

## Appendix C: Details of minimal MC calculation

### 1. Decomposition of $\psi^\sigma$ into active orbitals for the generic three-site model

The general decomposition of  $\psi^\uparrow$  and  $\psi^\downarrow$  should look as follows:

$$\begin{aligned}\psi^\uparrow &= c_1\phi_{M_1} + c_2\phi_{M_2} + c_g^o\phi_{lg}^o + c_u^o\phi_{lu}^o + c_g^e\phi_{lg}^e + c_u^e\phi_{lu}^e, \\ \psi^\downarrow &= c_2\phi_{M_1} + c_1\phi_{M_2} + c_g^o\phi_{lg}^o - c_u^o\phi_{lu}^o + c_g^e\phi_{lg}^e - c_u^e\phi_{lu}^e,\end{aligned}\quad (\text{C1})$$

where, compared to Eq. (10), the ungerade doubly occupied and gerade empty ligand active orbitals have been added for completeness:

$$\phi_{lu}^o = \sum_\mu a_{\mu u}\psi_{\mu u}, \quad \phi_{lg}^e = \sum_\mu a_{ig}\psi_{ig}. \quad (\text{C2})$$

Taking into account the orthonormality of the active ligand orbitals entering Eq. (C1) and their orthogonality to  $\phi_{M_1}$  and  $\phi_{M_2}$ , we calculate their overlaps with  $\psi^\sigma$  from which the expansion coefficients  $c_u^o$  and  $c_g^e$  are found to be zero, while  $c_g^o$  and  $c_u^e$  are given by Eq. (14).

The expansion coefficients  $c_1$  and  $c_2$  in Eq. (C1) are found by imposing the orthonormality on  $\phi_{M_1}$  and  $\phi_{M_2}$ :

$$\begin{aligned}c_{1,2} &= \frac{1}{2}\left(\sqrt{B+A} \pm \sqrt{B-A}\right), \\ B &= 1 - c_g^{o2} - c_u^{e2}, \\ A &= \frac{S_M - c_g^{o2} + c_u^{e2}}{B}.\end{aligned}\quad (\text{C3})$$

Thus, having in mind the relations (14), all expansion coefficients in Eq. (C1) depend on  $d_g^o$  and  $d_u^e$ .

Using Eq. (C3) we derive the active magnetic orbitals:

$$\begin{aligned}\phi_{M_{1,2}} &= \frac{(1 + S_M - d_g^{o2})\psi_o - b_g^o d_g^o \psi_{lg}^o}{(c_1 + c_2)\sqrt{2(1 + S_M)}} \\ &\pm \frac{(1 - S_M - d_u^{e2})\psi_e - d_u^e b_u^e \psi_{lu}^e}{(c_1 - c_2)\sqrt{2(1 - S_M)}}.\end{aligned}\quad (\text{C4})$$

Given the relations  $b_g^o = \sqrt{1 - d_g^{o2}}$ ,  $b_u^e = \sqrt{1 - d_u^{e2}}$  [see Eq. (11)] and Eqs. (14), the orbitals  $\phi_{M_{1,2}}$  are defined only through the coefficients  $d_g^o$  and  $d_u^e$ .

### 2. MC calculation in the electron-hole representation

For the restricted doubly occupied orbitals  $\psi_\mu$  we pass from electron to the hole representation. In the language of second quantization<sup>50</sup> the electron creation is replaced by hole annihilation and vice versa:

$$b_{\mu\sigma} = a_{\mu\sigma}^\dagger, \quad b_{\mu\sigma}^\dagger = a_{\mu\sigma}. \quad (\text{C5})$$

### a. Configuration functions in the electron-hole representation

Considering the determinant of restricted doubly occupied states, Eq. (19), as a vacuum function with respect to added holes (removed electrons),  $|0\rangle_h$ , while keeping the usual electronic representation for magnetic and restricted empty orbitals, with the vacuum function with respect to added electrons to these orbitals,  $|0\rangle_e$ , we can represent any determinant entering the configuration functions  $\Phi_I$  in (18) as products of few  $a_{i\sigma}^\dagger$  and  $b_{\mu\sigma}^\dagger$  operators acting on the vacuum function  $|0\rangle_e|0\rangle_h (\equiv |0\rangle)$ . The total number of these operators can differ from one product to another, however, the difference of electronic and hole creation operators is equal to  $N_m$  for each product.

For instance, the ground configuration in Fig. 4(b), described by the determinant

$$\Phi_1 = |\phi_{M_1}\bar{\phi}_{M_2}\phi_{lg}^o\bar{\phi}_{lg}^o\psi_1'\bar{\psi}'_1\cdots\psi_\mu'\bar{\psi}'_\mu\cdots|, \quad (\text{C6})$$

is written in the electron-hole representation as follows

$$\begin{aligned}\Phi_1 &= (\alpha a_{o\uparrow}^\dagger + \beta b_{lo\uparrow} + \gamma a_{e\uparrow}^\dagger + \delta a_{le\uparrow}^\dagger) \\ &(\alpha a_{o\downarrow}^\dagger + \beta b_{lo\downarrow} - \gamma a_{e\downarrow}^\dagger - \delta a_{le\downarrow}^\dagger)(b_g^o\beta b_{lo\uparrow} + d_g^o a_{o\uparrow}^\dagger) \\ &(b_g^o\beta b_{lo\downarrow} + d_g^o a_{o\downarrow}^\dagger)b_{lo\uparrow}^\dagger b_{lo\downarrow}^\dagger|0\rangle,\end{aligned}\quad (\text{C7})$$

where  $\alpha, \beta, \gamma, \delta$  are the coefficients in front of the corresponding orbital functions in (C4), the latter being replaced by corresponding electron creation and hole annihilation operators (the parity index was dropped for shortness); the coefficients  $d_g^o$  and  $b_g^o$  are the same as in Eq. (11).

The total density corresponding to  $\Phi_1$  can be written after making use of the relation (19) in the following form:

$$\begin{aligned}\rho^{\Phi_1}(\mathbf{r}) &= \sum_\mu^{\text{d.occ}} 2|\psi_\mu(\mathbf{r})|^2 - 2|\psi_{lg}^o(\mathbf{r})|^2 + 2|\phi_{lg}^o(\mathbf{r})|^2 \\ &+ |\phi_{M_1}(\mathbf{r})|^2 + |\phi_{M_2}(\mathbf{r})|^2,\end{aligned}\quad (\text{C8})$$

where the expressions of active orbitals via restricted and BS molecular orbitals are given by Eqs. (11)-(13) and (C4).

### b. The Hamiltonian in the electron-hole representation

In the electronic Hamiltonian

$$\hat{H} = \sum_{ij\sigma} h_{ij} a_{i\sigma}^\dagger a_{j\sigma} + \frac{1}{2} \sum_{ijkl} \sum_{\sigma\sigma'} V_{ijkl} a_{i\sigma}^\dagger a_{j\sigma'}^\dagger a_{l\sigma} a_{k\sigma'} \quad (\text{C9})$$

we pass to hole operators (C5) for restricted doubly occupied orbitals  $\psi_\mu$  and obtain:

$$\hat{H} = \hat{H}_a + \hat{H}_b + \hat{H}_{ab} + E_{\text{d.occ}}, \quad (\text{C10})$$

where  $\hat{H}_a$  is the electronic part given by Eq. (C9) in which the summations over orbital indices exclude the

orbitals  $\psi_\mu$ , and  $\hat{H}_b$  is the Hamiltonian for holes (in the following formulas the hole orbitals are denoted by Greek letters):

$$\begin{aligned} \hat{H}_b = & - \sum_{\mu\nu\sigma} [h_{\nu\mu} + \sum_{\kappa} (2V_{\nu\kappa\mu\kappa} - V_{\nu\kappa\kappa\mu})] b_{\mu\sigma}^\dagger b_{\nu\sigma} \\ & + \frac{1}{2} \sum_{\mu\nu\kappa\rho} \sum_{\sigma\sigma'} V_{\rho\kappa\nu\mu} b_{\mu\sigma}^\dagger b_{\nu\sigma'}^\dagger b_{\rho\sigma'} b_{\kappa\sigma}. \end{aligned} \quad (\text{C11})$$

The third term in (C10) is the mixed electron-hole part,

$$\begin{aligned} \hat{H}_{ab} = & \sum_{i\mu\sigma} h_{i\mu} (b_{\mu\sigma} a_{i\sigma} + a_{i\sigma}^\dagger b_{\mu\sigma}^\dagger) \\ & + \sum_{ijk\mu} \sum_{\sigma\sigma'} V_{ij\mu k} (a_{i\sigma}^\dagger a_{j\sigma'}^\dagger a_{k\sigma'} b_{\mu\sigma}^\dagger + b_{\mu\sigma} a_{k\sigma'}^\dagger a_{j\sigma'} a_{i\sigma}) \\ & + \sum_{i\mu\nu\kappa} \sum_{\sigma\sigma'} V_{ij\mu\kappa} (a_{i\sigma}^\dagger b_{\mu\sigma'}^\dagger b_{\nu\sigma'}^\dagger b_{\kappa\sigma}^\dagger + b_{\kappa\sigma} b_{\nu\sigma'}^\dagger b_{\mu\sigma'}^\dagger a_{i\sigma}) \\ & + \frac{1}{2} \sum_{ij\mu\nu} \sum_{\sigma\sigma'} V_{ij\mu\nu} (a_{i\sigma}^\dagger a_{j\sigma'}^\dagger b_{\nu\sigma'}^\dagger b_{\mu\sigma}^\dagger + b_{\mu\sigma} b_{\nu\sigma'}^\dagger a_{j\sigma'} a_{i\sigma}) \\ & + \sum_{ij\mu\nu} \sum_{\sigma\sigma'} (V_{i\mu\nu j} a_{i\sigma}^\dagger a_{j\sigma} b_{\mu\sigma'}^\dagger b_{\nu\sigma'}^\dagger - V_{i\mu\nu j} a_{i\sigma}^\dagger a_{j\sigma'} b_{\mu\sigma'}^\dagger b_{\nu\sigma}^\dagger), \end{aligned} \quad (\text{C12})$$

and the last one is the energy of the closed shell of restricted doubly occupied orbitals:

$$E_{d.\text{occ}} = 2 \sum_{\mu} h_{\mu\mu} + \sum_{\mu\mu'} (2V_{\mu\mu'\mu\mu'} - V_{\mu\mu'\mu'\mu}) \quad (\text{C13})$$

The above expressions were derived for real orbitals implying usual symmetry relations for matrix elements (indices refer to all orbitals):

$$h_{ij} = h_{ji}, \quad V_{ijkl} = V_{kjil} = V_{ilkj} = V_{klij} = \dots \quad (\text{C14})$$

In terms of canonical KS orbitals, the electronic Hamiltonian is obtained from (C9) via the following replacements:

$$\begin{aligned} i) \quad & h_{ij} \rightarrow \epsilon_i \delta_{ij}, \\ ii) \quad & \frac{1}{2} \sum_{ijkl} \sum_{\sigma\sigma'} V_{ijkl} a_{i\sigma}^\dagger a_{j\sigma'}^\dagger a_{l\sigma'} a_{k\sigma} \rightarrow \\ & \frac{1}{2} \sum_{ijkl} \sum_{\sigma\sigma'} V_{ijkl} (1 - 2\delta_{ij}) a_{i\sigma}^\dagger a_{j\sigma'}^\dagger a_{l\sigma'} a_{k\sigma} \\ & - \sum_{ij\sigma} [(v_c)_{ij} - (v_x)_{ij}] a_{i\sigma}^\dagger a_{j\sigma}, \end{aligned} \quad (\text{C15})$$

where is the KS orbital energy and  $v_c$  and  $v_x$  is the correlation and exchange potential, respectively. The electron-hole representation for this Hamiltonian is derived similarly to Eqs. (C10)-(C13).

<sup>1</sup>P. W. Anderson, "Theory of magnetic exchange interactions: exchange in insulators and semiconductors," in *Solid State Physics*, Vol. 14, edited by F. Seitz and D. Turnbull (Academic Press, New York, 1963) pp. 99–214.

<sup>2</sup>J. B. Goodenough, *Magnetism and the Chemical Bond* (Interscience, New York, 1963).

<sup>3</sup>A. P. Ginsberg, "Magnetic exchange in transition metal complexes vi: Aspects of exchange coupling in magnetic cluster complexes," *Inorg. Chim. Acta Rev.* **5**, 45 (1971).

<sup>4</sup>W. Geertsma, "Exchange interactions in insulators and semiconductors: I. the cation-anion-cation three-center model," *Physica B* **164**, 241 (1990).

<sup>5</sup>O. Kahn, *Molecular Magnetism* (VCH Publishers, New York, 1993).

<sup>6</sup>D. I. Khomskii, *Transition Metal Compounds* (Cambridge University Press, 2014).

<sup>7</sup>S. V. Streltsov and D. I. Khomskii, "Orbital physics in transition metal compounds: new trends," *Physics-Uspekhi* **60**, 1121 (2017).

<sup>8</sup>A. Ceulemans, L. F. Chibotaru, G. A. Heylen, K. Pierloot, and L. G. Vanquickenborne, "Theoretical Models of Exchange Interactions in Dimeric Transition-Metal Complexes," *Chemical Reviews* **100**, 787–806 (2000).

<sup>9</sup>E. Ruiz, "Theoretical Study of the Exchange Coupling in Large Polynuclear Transition Metal Complexes Using DFT Methods," in *Principles and Applications of Density Functional Theory in Inorganic Chemistry* (Springer Berlin Heidelberg, Berlin, Heidelberg, 2004) pp. 71–102.

<sup>10</sup>F. Neese, "Prediction of molecular properties and molecular spectroscopy with density functional theory: From fundamental theory to exchange-coupling," *Coord. Chem. Rev.* **253**, 526 (2009).

<sup>11</sup>H. Xiang, C. Lee, H.-J. Koo, X. Gong, and M.-H. Whangbo, "Magnetic properties and energy-mapping analysis," *Dalton Trans.* **42**, 823–853 (2013).

<sup>12</sup>K. Riedl, Y. Li, R. Valentí, and S. M. Winter, "Ab Initio Approaches for Low-Energy Spin Hamiltonians," *phys. status solidi (b)* **256**, 1800684 (2019).

<sup>13</sup>L. Noodleman, "Valence bond description of antiferromagnetic coupling in transition metal dimers," *J. Chem. Phys.* **74**, 5737 (1981).

<sup>14</sup>K. Yamaguchi, Y. Takahara, and T. Fueno, "Ab-initio molecular orbital studies of structure and reactivity of transition metal-oxo compounds," in *Applied Quantum Chemistry*, edited by V. H. Smith, H. F. Schaefer, and K. Morokuma (Springer Netherlands, Dordrecht, 1986) pp. 155–184.

<sup>15</sup>T. Soda, Y. Kitagawa, T. Onishi, Y. Takano, Y. Shigeta, H. Nagao, Y. Yoshioka, and K. Yamaguchi, "Ab initio computations of effective exchange integrals for H-H, H-He-H and Mn<sub>2</sub>O<sub>2</sub> complex: comparison of broken-symmetry approaches," *Chem. Phys. Lett.* **319**, 223 (2000).

<sup>16</sup>H. Schurkus, D.-T. Chen, H.-P. Cheng, G. Chan, and J. Stanton, "Theoretical prediction of magnetic exchange coupling constants from broken-symmetry coupled cluster calculations," *J. Chem. Phys.* **152**, 234115 (2020).

<sup>17</sup>A. Mansikkamäki, Z. Huang, N. Iwahara, and L. F. Chibotaru, "Broken symmetry  $G_0W_0$  approach for the evaluation of exchange coupling constants," (2020), [arXiv:2003.06334 \[cond-mat.str-el\]](https://arxiv.org/abs/2003.06334).

<sup>18</sup>P. Pokhilko and D. Zgid, "Broken-symmetry self-consistent GW approach: Degree of spin contamination and evaluation of effective exchange couplings in solid antiferromagnets," *The Journal of Chemical Physics* **157**, 144101 (2022).

<sup>19</sup>P. Pokhilko and D. Zgid, "Natural orbitals and two-particle correlators as tools for the analysis of effective exchange couplings in solids," *Phys. Chem. Chem. Phys.* **25**, 21267–21279 (2023).

<sup>20</sup>R. L. Martin and F. Illas, "Antiferromagnetic Exchange Interactions from Hybrid Density Functional Theory," *Phys. Rev. Lett.* **79**, 1539 (1997).

<sup>21</sup>E. Ruiz, P. Alemany, S. Alvarez, and J. Cano, "Toward the prediction of magnetic coupling in molecular systems: Hydroxo- and alkoxo-bridged cu(ii) binuclear complexes," *Journal of the American Chemical Society* **119**, 1297–1303 (1997).

- <sup>22</sup>A. Mansikkamäki, *Theoretical and computational studies of magnetic anisotropy and exchange coupling in molecular systems*, Ph.D. thesis (2018), University of Jyväskylä.
- <sup>23</sup>P. Rivero, I. d. P. R. Moreira, F. Illas, and G. E. Scuseria, “Reliability of range-separated hybrid functionals for describing magnetic coupling in molecular systems,” *The Journal of Chemical Physics* **129**, 184110 (2008).
- <sup>24</sup>R. Valero, R. Costa, I. de P. R. Moreira, D. G. Truhlar, and F. Illas, “Performance of the M06 family of exchange-correlation functionals for predicting magnetic coupling in organic and inorganic molecules,” *The Journal of Chemical Physics* **128**, 114103 (2008).
- <sup>25</sup>J. E. Peralta and J. I. Melo, “Magnetic Exchange Couplings with Range-Separated Hybrid Density Functionals,” *Journal of Chemical Theory and Computation* **6**, 1894–1899 (2010).
- <sup>26</sup>J. J. Phillips and J. E. Peralta, “The role of range-separated Hartree–Fock exchange in the calculation of magnetic exchange couplings in transition metal complexes,” *The Journal of Chemical Physics* **134**, 034108 (2011).
- <sup>27</sup>J. J. Phillips and J. E. Peralta, “Magnetic exchange couplings from semilocal functionals evaluated nonself-consistently on hybrid densities: Insights on relative importance of exchange, correlation, and delocalization,” *Journal of Chemical Theory and Computation* **8**, 3147–3158 (2012).
- <sup>28</sup>V. Polo, J. Gräfenstein, E. Kraka, and D. Cremer, “Long-range and short-range Coulomb correlation effects as simulated by Hartree–Fock, local density approximation, and generalized gradient approximation exchange functionals,” *Theor. Chem. Acc.* **109**, 22–35 (2003).
- <sup>29</sup>T. Glaser, T. Beissel, E. Bill, T. Weyhermüller, V. Schünemann, W. Meyer-Klaucke, A. X. Trautwein, and K. Wieghardt, “Electronic Structure of Linear Thiophenolate-Bridged Heterotrinnuclear Complexes [LFeMFeL]<sup>n+</sup> (M = Cr, Co, Fe; n = 1-3): Localized vs Delocalized Models,” *J. Am. Chem. Soc.* **121**, 2193 (1999).
- <sup>30</sup>F. Mizuno, H. Masuda, I. Hirabayashi, S. Tanaka, M. Hasegawa, and U. Mizutani, “Low-temperature ferromagnetism in La<sub>4</sub>Ba<sub>2</sub>Cu<sub>2</sub>O<sub>10</sub>,” *Science* **345**, 788 (1990).
- <sup>31</sup>H. Masuda, F. Mizuno, I. Hirabayashi, and S. Tanaka, “Electron-spin resonance and ferromagnetism in a copper oxide: La<sub>4</sub>Ba<sub>2</sub>Cu<sub>2</sub>O<sub>10</sub>,” *Phys. Rev. B* **43**, 7871 (1991).
- <sup>32</sup>L. F. Chibotaru, L. Ungur, C. Aronica, H. Elmoll, G. Pilet, and D. Luneau, “Structure, Magnetism, and Theoretical Study of a Mixed-Valence Co<sub>3</sub><sup>II</sup>Co<sub>4</sub><sup>III</sup> Heptanuclear Wheel: Lack of SMM Behavior despite Negative Magnetic Anisotropy,” *J. Am. Chem. Soc.* **130**, 12445 (2008).
- <sup>33</sup>Z. Huang, D. Liu, A. Mansikkamäki, V. Vieru, N. Iwahara, and L. F. Chibotaru, “Ferromagnetic kinetic exchange interaction in magnetic insulators,” *Phys. Rev. Res.* **2**, 033430 (2020).
- <sup>34</sup>P. W. Anderson, “New approach to the theory of superexchange interactions,” *Phys. Rev.* **115**, 2 (1959).
- <sup>35</sup>H. Tasaki, “Ferromagnetism in Hubbard Models,” *Phys. Rev. Lett.* **75**, 4678 (1995).
- <sup>36</sup>L. F. Chibotaru, J.-J. Girerd, G. Blondin, T. Glaser, and K. Wieghardt, “Ferromagnétisme et délocalisation électronique dans des complexes trimétalliques linéaires,” in *5ème Réunion des Chimistes Théoriciens Français* (1996).
- <sup>37</sup>L. F. Chibotaru, J.-J. Girerd, G. Blondin, T. Glaser, and K. Wieghardt, “Electronic Structure of Linear Thiophenolate-Bridged Heteronuclear Complexes [LFeMFeL]<sup>n+</sup> (M = Cr, Co, Fe; n = 1-3): A Combination of Kinetic Exchange Interaction and Electron Delocalization,” *J. Am. Chem. Soc.* **125**, 12615 (2003).
- <sup>38</sup>K. Penc, H. Shiba, F. Mila, and T. Tsukagoshi, “Ferromagnetism in multiband Hubbard models: From weak to strong Coulomb repulsion,” *Phys. Rev. B* **54**, 4056 (1996).
- <sup>39</sup>H. Tasaki, *Physics and mathematics of quantum many-body systems* (Springer International Publishing, 2020).
- <sup>40</sup>Precisely,  $t'$  is compared with  $t^2/\Delta$  ( $\Delta \gg |t|, |t'|$ )<sup>33</sup>. When they are comparable, their influence on the exchange interaction is similar.
- <sup>41</sup>Although the model (1) provides a potential exchange contribution when one passes from the Wannier orbitals 1, 2 and  $l$  to the magnetic orbitals of Anderson’s type<sup>88</sup>, appreciable direct potential exchange interaction can already exist for the localized orbitals 1 and 2 in many magnetic materials<sup>33</sup>. For simplicity, we do not include this interaction in the model (1) since it does not influence the main conclusions of this work.
- <sup>42</sup>In the *ab initio* calculations of complexes, contrary to the HF method, the DFT calculations partly include the electron correlation through the exchange-correlation functional, an effect more pronounced for pure than hybrid functionals<sup>70</sup>. This effect is accounted for by the denominator of Yamaguchi’s expression which is simply proved by the fact that in the limit of exact exchange-correlation functional, when  $\langle \hat{S}^2 \rangle_{\text{BS-DFT}} = 0$ , the corresponding Eq. (3) will correctly describe the energy difference between two states with definite spin.
- <sup>43</sup>A. I. Liechtenstein, M. I. Katsnelson, V. P. Antropov, and V. A. Gubanov, “Local spin density functional approach to the theory of exchange interactions in ferromagnetic metals and alloys,” *J. Magn. Magn. Mater.* **67**, 65 (1987).
- <sup>44</sup>One may think that the breakdown of the BS approach may be cured by using a spin symmetry adapted state instead of the UHF state (see Appendix A 2 c). We confirm with our toy model that such an approach is far from satisfactory in reproducing the exact  $J$ . To improve the BS approach, the use of a multiconfigurational approach is decisive. In practice, similar attempts have been made using DFT, while clear improvement of  $J$  of real molecules has not been seen<sup>86</sup>.
- <sup>45</sup>L. Noodleman, T. Lovell, T. Liu, F. Himo, and R. A. Torres, “Insights into properties and energetics of iron–sulfur proteins from simple clusters to nitrogenase,” *Current Opinion in Chemical Biology* **6**, 259 – 273 (2002).
- <sup>46</sup>J. P. Malrieu, R. Caballol, C. J. Calzado, C. de Graaf, and N. Guihéry, “Magnetic Interactions in Molecules and Highly Correlated Materials: Physical Content, Analytical Derivation, and Rigorous Extraction of Magnetic Hamiltonians,” *Chem. Rev.* **114**, 429–492 (2013).
- <sup>47</sup>R. Caballol, O. Castell, F. Illas, I. de P. R. Moreira, and J. P. Malrieu, “Remarks on the proper use of the broken symmetry approach to magnetic coupling,” *J. Phys. Chem. A* **101**, 7860–7866 (1997).
- <sup>48</sup>In the case when the complex possesses a two-fold rotational symmetry interchanging the magnetic centres, the indices  $g$  and  $u$  are replaced by the irreducible representations  $a_1$  and  $a_2$  of the  $C_2$  symmetry group, respectively.
- <sup>49</sup>N. Marzari, A. A. Mostofi, J. R. Yates, I. Souza, and D. Vanderbilt, “Maximally localized Wannier functions: Theory and applications,” *Rev. Mod. Phys.* **84**, 1419–1475 (2012).
- <sup>50</sup>R. McWeeny, *Methods of Molecular Quantum Mechanics* (Academic Press, London, 1989).
- <sup>51</sup>B. O. Roos, R. Lindh, P. Åke Malmqvist, V. Veryazov, and P. Widmark, *Multiconfigurational Quantum Chemistry* (John Wiley & Sons, Inc., New Jersey, 2016).
- <sup>52</sup>M. Weimer, F. Della Sala, and A. Görling, “Multiconfiguration optimized effective potential method for a density-functional treatment of static correlation,” *J. Chem. Phys.* **128**, 144109 (2008).
- <sup>53</sup>Y. Kurzwil, K. V. Lawler, and M. Head-Gordon, “Analysis of multi-configuration density functional theory methods: theory and model application to bond-breaking,” *Mol. Phys.* **107**, 2103–2110 (2009).
- <sup>54</sup>R. Pollet, A. Savin, T. Leininger, and H. Stoll, “Combining multideterminantal wave functions with density functionals to handle near-degeneracy in atoms and molecules,” *J. Chem. Phys.* **116**, 1250–1258 (2002).
- <sup>55</sup>K. Sharkas, A. Savin, H. J. A. Jensen, and J. Toulouse, “A multiconfigurational hybrid density-functional theory,” *J. Chem. Phys.* **137**, 044104 (2012).



- <sup>56</sup>E. Fromager, R. Cimiraglia, and H. J. A. Jensen, "Merging multireference perturbation and density-functional theories by means of range separation: Potential curves for Be<sub>2</sub>, Mg<sub>2</sub>, and Ca<sub>2</sub>," *Phys. Rev. A* **81**, 024502 (2010).
- <sup>57</sup>J. Gräfenstein and D. Cremer, "The combination of density functional theory with multi-configuration methods – CAS-DFT," *Chem. Phys. Lett.* **316**, 569–577 (2000).
- <sup>58</sup>J. Gräfenstein and D. Cremer, "Development of a CAS-DFT method covering non-dynamical and dynamical electron correlation in a balanced way," *Mol. Phys.* **103**, 279–308 (2005).
- <sup>59</sup>R. Takeda, S. Yamanaka, and K. Yamaguchi, "CAS-DFT based on odd-electron density and radical density," *Chem. Phys. Lett.* **366**, 321–328 (2002).
- <sup>60</sup>S. Yamanaka, K. Nakata, T. Ukai, T. Takada, and K. Yamaguchi, "Multireference density functional theory with orbital-dependent correlation corrections," *Int. J. Quantum Chem.* **106**, 3312–3324 (2006).
- <sup>61</sup>T. Ukai, K. Nakata, S. Yamanaka, T. Kubo, Y. Morita, T. Takada, and K. Yamaguchi, "CASCI-DFT study of the phenalenyl radical system," *Polyhedron* **26**, 2313–2319 (2007).
- <sup>62</sup>Y. Zhao, B. J. Lynch, and D. G. Truhlar, "Doubly hybrid meta dft: New multi-coefficient correlation and density functional methods for thermochemistry and thermochemical kinetics," *J. Phys. Chem. A* **108**, 4786–4791 (2004).
- <sup>63</sup>Y. Zhao, B. J. Lynch, and D. G. Truhlar, "Multi-coefficient extrapolated density functional theory for thermochemistry and thermochemical kinetics," *Phys. Chem. Chem. Phys.* **7**, 43–52 (2005).
- <sup>64</sup>S. Grimme and M. Waletzke, "A combination of Kohn–Sham density functional theory and multi-reference configuration interaction methods," *J. Chem. Phys.* **111**, 5645–5655 (1999).
- <sup>65</sup>M. Filatov and S. Shaik, "A spin-restricted ensemble-referenced Kohn–Sham method and its application to diradicaloid situations," *Chem. Phys. Lett.* **304**, 429–437 (1999).
- <sup>66</sup>M. Filatov and S. Shaik, "Diradicaloids: Description by the Spin-Restricted, Ensemble-Referenced Kohn–Sham Density Functional Method," *J. Phys. Chem. A* **104**, 6628–6636 (2000).
- <sup>67</sup>M. Filatov, "Spin-restricted ensemble-referenced Kohn–Sham method: basic principles and application to strongly correlated ground and excited states of molecules," *WIREs Comput. Mol. Sci.* **5**, 146–167 (2015).
- <sup>68</sup>M. Roemelt and F. Neese, "Excited States of Large Open-Shell Molecules: An Efficient, General, and Spin-Adapted Approach Based on a Restricted Open-Shell Ground State Wave function," *J. Phys. Chem. A* **117**, 3069–3083 (2013).
- <sup>69</sup>D. Maganas, M. Roemelt, T. Weyhermuller, R. Blume, M. Havecker, A. Knop-Gericke, S. DeBeer, R. Schlögl, and F. Neese, "L-edge X-ray absorption study of mononuclear vanadium complexes and spectral predictions using a restricted open shell configuration interaction ansatz," *Phys. Chem. Chem. Phys.* **16**, 264–276 (2014).
- <sup>70</sup>D. Cremer, M. Filatov, V. Polo, E. Kraka, and S. Shaik, "Implicit and Explicit Coverage of Multi-reference Effects by Density Functional Theory," *Int. J. Mol. Sci.* **3**, 604–638 (2002).
- <sup>71</sup>A. D. Becke, A. Savin, and H. Stoll, "Extension of the local-spin-density exchange-correlation approximation to multiplet states," *Theor. Chim. Acta* **91**, 147 (1995).
- <sup>72</sup>R. Colle and O. Salvetti, "Approximate calculation of the correlation energy for the closed shells," *Theor. Chim. Acta* **37**, 329–334 (1975).
- <sup>73</sup>R. Colle and O. Salvetti, "Generalization of the Colle-Salvetti correlation energy method to a many-determinant wave function," *J. Chem. Phys.* **93**, 534–544 (1990).
- <sup>74</sup>C. Lee, W. Yang, and R. G. Parr, "Development of the Colle-Salvetti correlation-energy formula into a functional of the electron density," *Phys. Rev. B* **37**, 785–789 (1988).
- <sup>75</sup>G. Li Manni, R. K. Carlson, S. Luo, D. Ma, J. Olsen, D. G. Truhlar, and L. Gagliardi, "Multiconfiguration Pair-Density Functional Theory," *J. Chem. Theory Comput.* **10**, 3669–3680 (2014).
- <sup>76</sup>L. Gagliardi, D. G. Truhlar, G. Li Manni, R. K. Carlson, C. E. Hoyer, and J. L. Bao, "Multiconfiguration Pair-Density Functional Theory: A New Way To Treat Strongly Correlated Systems," *Acc. Chem. Res.* **50**, 66–73 (2017).
- <sup>77</sup>I. Fdez. Galván, M. Vacher, A. Alavi, C. Angeli, F. Aquilante, J. Autschbach, J. J. Bao, S. I. Bokarev, N. A. Bogdanov, R. K. Carlson, L. F. Chibotaru, J. Creutzberg, N. Dattani, M. G. Delcey, S. S. Dong, A. Dreuw, L. Freitag, L. M. Frutos, L. Gagliardi, F. Gendron, A. Giussani, L. González, G. Grell, M. Guo, C. E. Hoyer, M. Johansson, S. Keller, S. Knecht, G. Kovačević, E. Källman, G. Li Manni, M. Lundberg, Y. Ma, S. Mai, J. P. Malhado, P. r. Malmqvist, P. Marquetand, S. A. Mewes, J. Norell, M. Olivucci, M. Oppel, Q. M. Phung, K. Pierloot, F. Plasser, M. Reiher, A. M. Sand, I. Schapiro, P. Sharma, C. J. Stein, L. K. Sørensen, D. G. Truhlar, M. Ugandi, L. Ungur, A. Valentini, S. Vancoillie, V. Veryazov, O. Weser, T. A. Wesolowski, P.-O. Widmark, S. Wouters, A. Zech, J. P. Zobel, and R. Lindh, "Openmolcas: From source code to insight," *Journal of Chemical Theory and Computation* **15**, 5925–5964 (2019).
- <sup>78</sup>D. Presti, S. J. Stoneburner, D. G. Truhlar, and L. Gagliardi, "Full Correlation in a Multiconfigurational Study of Bimetallic Clusters: Restricted Active Space Pair-Density Functional Theory Study of [2Fe–2S] Systems," *J. Phys. Chem. C* **123**, 11899–11907 (2019).
- <sup>79</sup>J. L. Bao, A. Sand, L. Gagliardi, and D. G. Truhlar, "Correlated-Participating-Orbitals Pair-Density Functional Method and Application to Multiplet Energy Splittings of Main-Group Divalent Radicals," *J. Chem. Theory Comput.* **12**, 4274–4283 (2016).
- <sup>80</sup>S. J. Stoneburner, D. G. Truhlar, and L. Gagliardi, "MC-PDFT can calculate singlet–triplet splittings of organic diradicals," *J. Chem. Phys.* **148**, 064108 (2018).
- <sup>81</sup>P. Sharma, V. Bernales, S. Knecht, D. G. Truhlar, and L. Gagliardi, "Density matrix renormalization group pair-density functional theory (DMRG-PDFT): singlet–triplet gaps in polyacenes and polyacetylenes," *Chem. Sci.* **10**, 1716–1723 (2019).
- <sup>82</sup>C. Zhou, L. Gagliardi, and D. G. Truhlar, "Multiconfiguration Pair-Density Functional Theory for Iron Porphyrin with CAS, RAS, and DMRG Active Spaces," *J. Phys. Chem. A* **123**, 3389–3394 (2019).
- <sup>83</sup>S. J. Stoneburner, D. G. Truhlar, and L. Gagliardi, "Transition Metal Spin-State Energetics by MC-PDFT with High Local Exchange," *J. Phys. Chem. A* **124**, 1187–1195 (2020).
- <sup>84</sup>Y. Takano, T. Taniguchi, H. Isobe, T. Kubo, Y. Morita, K. Yamamoto, K. Nakasuji, T. Takui, and K. Yamaguchi, "Effective exchange integrals and chemical indices for a phenalenyl radical dimeric pair," *Chem. Phys. Lett.* **358**, 17–23 (2002).
- <sup>85</sup>A. J. Pérez-Jiménez, J. M. Pérez-Jordá, I. d. P. R. Moreira, and F. Illas, "Merging multiconfigurational wavefunctions and correlation functionals to predict magnetic coupling constants," *J. Comput. Chem.* **28**, 2559–2568 (2007).
- <sup>86</sup>I. de P. R. Moreira, R. Costa, M. Filatov, and F. Illas, "Restricted Ensemble-Referenced Kohn–Sham versus Broken Symmetry Approaches in Density Functional Theory: Magnetic Coupling in Cu Binuclear Complexes," *J. Chem. Theory Comput.* **3**, 764–774 (2007).
- <sup>87</sup>T. Leyser de Costa Gouveia, D. Maganas, and F. Neese, "General spin-restricted open-shell configuration interaction approach: Application to metal k-edge x-ray absorption spectra of ferro- and antiferromagnetically coupled dimers," *J. Phys. Chem. A* **XXX**, XXX–XXX (2025).
- <sup>88</sup>W. Van den Heuvel and L. F. Chibotaru, "Basic exchange model: Comparison of Anderson and valence bond configuration interaction approaches and an alternative exchange expression," *Phys. Rev. B* **76**, 104424 (2007).